Hindawi
Advances in Materials Science and Engineering
Volume 2021, Article ID 9954504, 12 pages
https://doi.org/10.1155/2021/9954504

Research Article

Freeze-Thaw Splitting Strength Analysis of PAC Based on the Gray-Markov Model

Baoyang Yu,[1,2] **Zongguang Sun**,[1] **and Lin Qi**[3]

[1]*Transportation Engineering College, Dalian Maritime University, Dalian 116026, China*
[2]*School of Traffic Engineering, Shenyang Jianzhu University, Shenyang 110168, China*
[3]*Department of Civil Engineering, Shenyang Urban Construction Institute, Shenyang 110167, China*

Correspondence should be addressed to Lin Qi; qilin6126@126.com

Received 9 March 2021; Accepted 30 July 2021; Published 6 August 2021

Academic Editor: Dimitrios E. Manolakos

In this study, a freeze-thaw split test was carried out to simulate the frost-heaving behavior of permeable asphalt concrete (PAC). Furthermore, the water stability problems caused by spalling and loosening were studied. Through a comparative analysis of the freeze-thaw split ratio of porosities of 19%, 21%, and 24%, the PAC porosity with excellent water stability was determined to be 19–21%. Scanning electron microscopy (SEM) images of PAC with the three porosity values after repeated freezing and thawing verified that the porosities were greater than 24% and the asphalt film peeling area was the largest, resulting in the rapid decline of the PAC freeze-thaw split ratio. The Gray-Markov model was used to predict the water stability of the mixture with a porosity of 21%. Based on the results, a Gray-Markov method for evaluating the PAC water stability in seasonally frozen areas was introduced.

1. Introduction

Compared with ordinary close-graded asphalt concrete, permeable asphalt concrete (PAC) has several advantages, including improved road drainage, an effective reduction in water mist due to the road-surface water accumulation, reduced noise, and reduced road surface temperature [1–4]. The characteristics of the drainage methods of PAC compared to those of ordinary fine-graded asphalt mixture are different. Water can be oozing down the pores to the drainage system, and the permeable system has a unified target in the application. However, PAC presents fewer fine aggregates, and the bond between the asphalt and the aggregate is more susceptible to environmental effects, such as freezing and thawing, leading to premature road surface damage [5, 6]. Especially in seasonally frozen areas, PAC undergoes multiple freeze-thaw cycles; thus, water stability should be substantially tested. Owing to its large porosity, PAC increases the possibility of freeze-thaw damage, which may cause loosening and flaking of the mixture, decreasing the performance. Otherwise, the porosity of the mixture is substantially small, and the water entering the mixture cannot be discharged in a timely manner, affecting the use of the permeable pavement. Therefore, by selecting a suitable porosity, the PAC water damage can be minimized, and the water stability can be improved. Currently, researchers often use high-viscosity modified asphalt and fiber blending to study the durability of PACs indoors and infields [7–9]. Zhang and Hu [10] prepared composite-modified asphalt by adding different plasticizers and cross-linking agents to improve the road performance of high-viscosity mixture (HVM), especially PAC durability. Wang et al. [11] studied how fiber affects the road performance of open-graded friction course (OGFC) based on the OGFC composition characteristics. The results showed that the addition of fiber could improve the high-temperature, low-temperature, and water stabilities. Moreover, lignin fiber had the best effect on the long-term improvement in OGFC water stability. In summary, PAC is not only a good pavement structural design but also an antifatigue material. On this basis, the pavement maintenance is carried out to extend the service life of the pavement.

There are several methods for predicting pavement performance deterioration. As frozen rain cannot be cleaned

in time and road icing will affect traffic safety, Xu et al. [12] used a backpropagation neural network method and local temperature data to establish a prediction model of the asphalt pavement temperature in frozen zones. The results showed that the model overcame the inaccuracy of the daily change point prediction and accurately predicted the road surface temperature in the next 3 h [12, 13]. However, because of the regional sample particularity, the method cannot be implemented in a wide range of areas. Park et al. [14] collected a large amount of regional data through the Texas Transportation Institute and used Bayesian methods to predict longitudinal cracks in Texas, USA. The research showed that the prediction performance was adequate and that the ability to predict the road surface damage was improved, thus saving a large amount of road maintenance budget. However, each pavement sample needs to be analyzed individually, and the approach required accurate data accumulated from many years of testing. Du and Cross [15] applied the gray prediction model to predict the rut depth of the asphalt pavement to solve the problem of large fluctuations of the pavement performance due to uncertain factors. By comparing the results with those from field test data, the error of the actual measured and predicted rut depths was determined to be within 2.5 mm, showing practicality with fewer sample numbers; however, from long-term forecast data, the prediction accuracy degraded, which did not contribute to the long-term prediction of the pavement performance. Based on the Markov state transition matrix of the crack and deformation areas, Abaza [16] predicted the degree of damage of the pavement section. The results showed that the length method had higher prediction accuracy and fewer interference factors than the area method and could be applied to the long-term maintenance and management of road surfaces. The Markov model is only affected by the current state, and the past state does not affect future characteristics. Markov theory has been successfully applied in fields such as bridges, pavement performance, and wastewater systems [17–19]; however, few applications exist in PAC.

Therefore, in this study, based on the porosity index of the mixture, three groups of freeze-thaw cycles with different porosities were developed. Then, specimens under different cycles were scanned using a scanning electron microscope (SEM). Afterwards, the applicability of each prediction model was comprehensively considered by analyzing experimental data. Subsequently, the advantages of the short-term prediction of the gray theory and the characteristics of the Markov prediction model were combined without after-effects. Finally, a combined prediction model based on the Gray-Markov theory was established to predict the PAC water stability performance.

2. Theoretical Research

2.1. Gray-Markov Model. The Markov prediction model is a probability prediction model whose prediction results are only related to the current state. The prediction model has no after-effects and is suitable for long-term prediction with large volatility and several uncertain factors [20].

Let the system have m states. If the probability of being in state i in the future is only related to the current state, then the conditional probability of the Markov chain is given as follows:

$$P_{ij}(n) = P\left(X_{n+1} = j \mid X_0 = x_0, X_1 = x_1 \cdots X_n = i\right) = P\left(X_{n+1} = j \mid X_n = i\right), \tag{1}$$

where $X_0 = x_0, X_1 = x_1 \cdots X_n = i$ represent all previous states of the system.

All possible transition probabilities for each state in the system are grouped into a matrix, which represents the transition probability matrix. The number of transitions from state E_i to state E_j is m_{ij}. The total number of occurrences of the transition from state E_i is M_{ij}. The state transition probability p_{ij} from state E_i to state E_j is recorded as m_{ij}/M_{ij}.

$$P = \begin{bmatrix} p_{11} & p_{12} & \cdots & p_{1n} \\ p_{11} & p_{12} & \cdots & p_{1n} \\ \vdots & \vdots & \vdots & \vdots \\ p_{m1} & p_{m2} & \cdots & p_{mn} \end{bmatrix}, \tag{2}$$

$$p_n = p_{n-1} \cdot p = p_0 \cdot p_n,$$

$$p_{ij} \geq 0 \sum_{i=1}^{m} p_{ij} = 1.$$

The test conditions and materials used in this study are typical, and the number of samples is small. The Markov model is used to check whether the sample information can represent the overall distribution. The specific calculation process of the Markov test standard can be obtained using the two following equations:

$$P_{\cdot j} = \frac{\sum_{i=1}^{3} m_{ij}}{\sum_{i=1}^{3} \sum_{j=1}^{3} m_{ij}}, \tag{3}$$

$$\chi^2 = 2 \sum_{i=1}^{3} \sum_{j=1}^{3} m_{ij} \left| \ln \frac{p_{ij}}{p_{\cdot j}} \right| > \chi_{\alpha}^2 (n+1), \tag{4}$$

where n refers to the number of Markov model division states. A significant level α refers to the probability that a sample can replace the overall distribution.

The Markov modified equation is as follows:

$$\widetilde{X}_{(k)} = \frac{1}{2} \times \left(\frac{\hat{X}_{(k)}}{1 - \varepsilon_1(k)} + \frac{\hat{X}_{(k)}}{1 - \varepsilon_2(k)} \right), \tag{5}$$

where $\widetilde{X}_{(k)}$ is fitted to the prediction value of the Markov model; $\varepsilon_1(k)$ and $\varepsilon_2(k)$ are the left and right endpoint values of the state interval where the sequence value is located, respectively.

Considering the advantages of the two models, we selected the Gray-Markov model. The main calculation idea is as follows. First, the gray prediction model is built using the measured data, and the prediction equation is calculated. Through the relative residual value, the PAC water stability grade is divided, the state transition matrix is determined, and the Markov test for the water stability is performed. Finally, the fitting prediction value of the gray model is corrected.

2.2. Gray Prediction Model. A smooth data sequence $Y_{(k)}$ is obtained from the original data sequence $X_{(i)}$ after one accumulation:

$$Y_{(k)} = \sum_{i=1}^{k} X_{(i)}, \tag{6}$$

and $Z_{(k)}$ is the average value of $Y_{(k)}$,

$$Z_{(k)} = \frac{1}{2}\left(Y_{(k)} + Y_{(k-1)}\right). \tag{7}$$

Next, a first-order linear differential equation is established:

$$\frac{\mathrm{d}Y}{\mathrm{d}k} + aY_{(k)} = b. \tag{8}$$

A solution is obtained using the constant coefficient variation method, where a and b are the spending parameters.

$$Y_{(k+1)} = \left[X_{(1)} - \frac{b}{a}\right]e^{-ak} + \frac{b}{a}. \tag{9}$$

The parameter vector is obtained by using the least-square method as follows:

$$\begin{aligned} Y_N &= \left[X_{(2)},\ X_{(3)}\ \cdots\ X_{(n)}\right]^{\mathrm{T}}, \\ B^{\mathrm{T}} &= \begin{bmatrix} -Z_{(2)} & -Z_{(3)} & \cdots & -Z_{(n)} \\ 1 & 1 & \cdots & 1 \end{bmatrix}, \\ \hat{a} &= \begin{bmatrix} a \\ b \end{bmatrix} = \left(B^{\mathrm{T}}B\right)^{-1}B^{\mathrm{T}}Y_N. \end{aligned} \tag{10}$$

Afterwards, parameters a and b are substituted into equation (2) to obtain the predicted value of the accumulated data as follows:

$$\hat{Y}_{(k+1)} = \left(X_{(1)} - \frac{b}{a}\right)e^{-ak} + \frac{b}{a}. \tag{11}$$

The gray predictions are restored by inverse subtraction:

$$\hat{X}_{(k+1)} = \hat{Y}_{(k+1)} - \hat{Y}_{(k)}. \tag{12}$$

The residual is given by

$$q(k) = X_{(k)} - \hat{X}_{(k)}. \tag{13}$$

Finally, the relative value of the residual is as follows:

$$\varepsilon(k) = \frac{q(k)}{X_{(k)}} \times 100\%. \tag{14}$$

3. Test Verification

3.1. Raw Materials. In general, PAC has a long contact with water over time. Under the action of traffic load, the adhesion of coarse and fine aggregates and binders in the mixture deteriorates. Moreover, looseness and stripping problems will be accelerated, eventually causing damage to the road surface. The water absorption of coarse aggregates substantially affects the low-temperature and water stabilities of PAC [21]. Therefore, when selecting a coarse aggregate, under the premise that other indicators satisfy the requirements, the water absorption index should be considered. In this study, the coarse aggregate was limestone with a water absorption of 0.93%. The types of fine aggregates included machine sand, natural sand, and stone chips. The surface roughness of natural sand is small, and the adhesion to asphalt is weak. The content of stone chips was substantially high and flat and difficult to compact. The surface of machine sand was rough and hard, with excellent angularity. Note that the adhesion between asphalt and stone is related to the acidity and alkalinity of the stone [22]. Thus, the fine aggregate was made of alkaline mechanical sand. Liaohe 90# asphalt was selected as the matrix asphalt. The modifier was a domestic high-viscosity OLB-1 modifier with a light yellow translucent spherical particles appearance. The addition of the modifier has multiple improvement effects on the matrix asphalt, such as reinforcement, thickening, and antiaging. The amount of modifier added via the external blending method was 12%. All indicators are tested on high-viscosity asphalt, which satisfied the requirements.

3.2. Gradation Design of the Mixture. The PAC design requires not only the embedded and stable mineral aggregate skeleton structure to meet ideal performance mixture requirements but also the ideal porosity to meet the drainage needs of the structure. This design concept is consistent with the coarse aggregate void filling method. Based on this method, the coarse aggregate was completely embedded and extruded while ensuring that the asphalt mortar entirely filled the main skeleton gap. The design gradation of the mixture in this study is shown in Figure 1.

A mineral gradation with better drainage function and preferable performance, such as the OGFC-13 gradation of the Liuqian Expressway in Anhui Province, China, should be selected to formulate the design gradation range of PAC. According to the gradation, 4.5%, 5.1%, and 5.7% of the oil-stone ratio were selected and mixed into test pieces, and the porosities were 19%, 21%, and 24%, respectively.

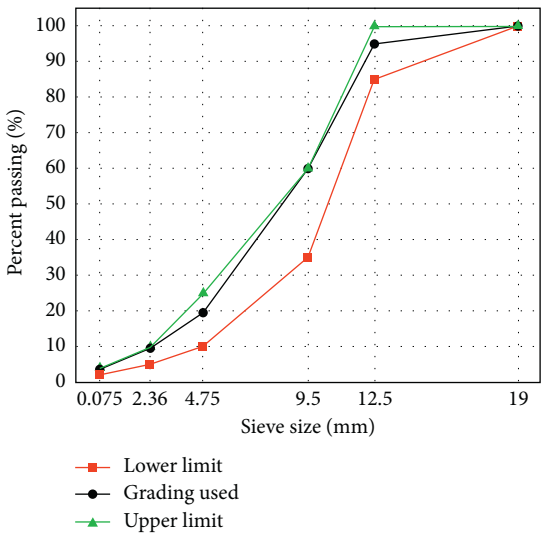

Figure 1: Results of the gradation composition of PAC (OGFC-13).

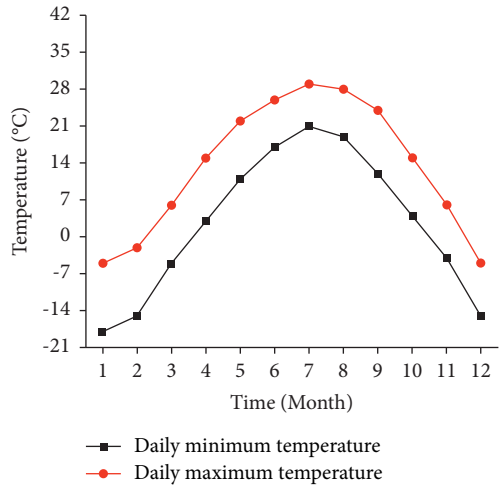

Figure 2: Annual temperature curve of Shenyang City.

3.3. Test Plan. The freeze-thaw damage of PAC is mainly caused by repeated freezing and thawing of the water inside the pavement [23]. During the early winter and early spring seasons in frozen zones, when the temperature drops below 0°C and the water phase in the pavement gap changes from liquid to solid, as well as liquid coexisting state to liquid state, PAC undergoes freeze-thaw cycles. For instance, in Shenyang City, in the Chinese seasonally frozen area, the daily average minimum temperature in November is lower than 0°C, and the daily maximum temperature in March is higher than 0°C. The pavement structure undergoes the cyclical effect of freezing and thawing. The specific temperature of Shenyang City is shown in Figure 2.

Previous studies have shown that the PAC water stability can be evaluated via the Marshall test and the freeze-thaw split test under water immersion conditions. The test conditions were as follows. The test specimen was immersed in a 60°C water bath at atmospheric pressure. The freeze-thaw cycle condition was vacuuming in a −18°C low-temperature box for 18 h, removing, and then thawing in a 60°C water bath for 24 h. The freezing and thawing effects of the road surface in winter and spring were simulated, and the number of cycles was different. Different test instruments and indicators were used for the analysis depending on the purpose [24, 25]. According to the comparative analysis of the above-mentioned water stability evaluation methods combined with the characteristics of urban temperature in the seasonally frozen area, the freeze-thaw split test was conducted in this study. The gradation type was OGFC-13. Specimens were formed by creating a cylinder with a height of 63.5 mm and a diameter of 100 mm, compacting 50 times. The vacuum freezing method was adopted to fill the porosity of the mixture with water completely, and the limit temperature of the low-temperature freezing setting was −30°C. The temperature difference between cold and heat settings was large enough so that the mixture reached the most unfavorable state. Moreover, the actual engineering condition of PAC was simulated. The conditions of freeze-thaw cycles were as follows: vacuum saturation for 15 min, soaking for 30 min, freezing at −18°C for 12 h, and thawing in a 60°C water bath for 4 h, in addition to freezing at −18°C for 4 h, thawing in a 60°C water bath for 4 h, freezing at −18°C for 12 h, thawing in a 60°C water bath for 4 h, freezing at −30°C for 4 h, and thawing in a 60°C water bath for 4 h. The number of freeze-thaw cycles ranged from 0 to 20 in intervals of two.

Using the new freeze-thaw cycle method, the freeze-thaw splitting tests were carried out on PAC samples with porosities of 19%, 21%, and 24%. The specific test process is shown in Figure 3, and the results are shown in Figure 4.

Figure 4 shows that when PAC with a porosity of 24% underwent 20 freeze-thaw cycles, the decrease in the tensile strength ratio (TSR) was the largest among the different porosities. The main reason was that the asphalt content was low and that the porosity in this specimen was large compared to those in specimens with different porosities. After vacuum saturation, the moisture content in the gap was relatively large. Simultaneously, as the number of freeze-thaw cycles was increased, the porosity of the mixture increased, and more water entered and gradually infiltrated between the asphalt and the mineral material, as well as the gap between the mineral material and the aggregate. The adhesion between the asphalt and the mineral material was weakened due to the increased water concentration in the gap, resulting in poor water stability of the mixture. After 20 freeze-thaw cycles, the water stabilities of PAC with porosities of 19% and 21% were approximately the same; however, that with a porosity of 21% was slightly better than that with a porosity of 19%. Through the analysis presented above, when the porosity of PAC was controlled between 19% and 21%, a preferable water damage resistance of the permeable pavement could be achieved.

3.4. SEM Experiment. To verify the results of the freeze-thaw splitting test, we investigated the micromorphology of the mixture. In this regard, SEM images of the mixture of the three porosities after multiple freeze-thaw cycles were obtained.

(a) (b)

Figure 3: Process of freezing and thawing the test samples. Specimen appearance (a) after freezing and (b) after melting.

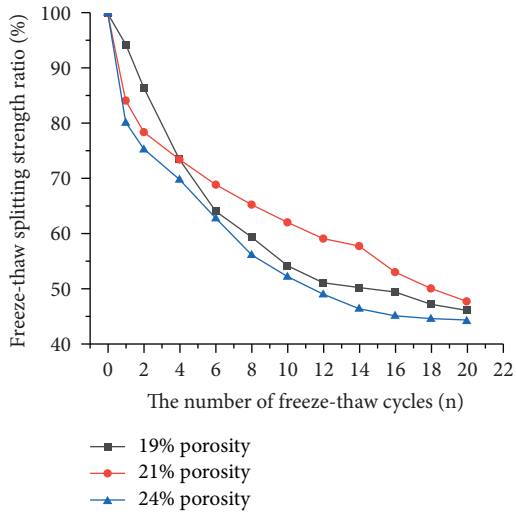

Figure 4: Variation diagram of the specimens' tensile strength ratio for different porosities.

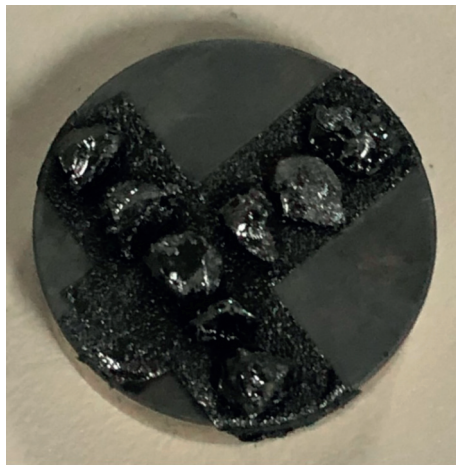

Figure 5: Specimens after the gold spraying process.

The ImageJ software was used to extract the peeling area of the asphalt film, and the law of the peeling area of the asphalt film with the freeze-thaw cycle was analyzed, which provided a basis for the evaluation of the previous macroscopic results.

Samples were taken from the test specimens that underwent different freeze-thaw cycles. The sample was cut out with a diameter of approximately 0.3–0.5 cm from the inside of the test specimen. The sample was fixed on the stage with a special fixing device, and gold powder was sprayed on the sample to facilitate the observation of the structure surface. Figure 5 shows the gold-sprayed instrument and the gold-sprayed specimens. Figures 6–8 show SEM images (500x magnification) of the samples under multiple freeze-thaw cycles.

Figures 6–8 show that, when not frozen and thawed, the asphalt film was smooth and not punctured by aggregates. After two freeze-thaw cycles, the asphalt film peels off in a small area. The main reason is that the freeze-thaw effect makes the asphalt brittle, and the action of the ice heaving force causes certain damage to the asphalt interface. With an increase in the number of freeze-thaw cycles, the aggregate develops further, punctures the asphalt membrane, and then develops deep-seated cracking of the asphalt membrane with a net-like tendency.

The qualitative processing of the SEM images mentioned above cannot quantitatively evaluate the degree of delamination of the asphalt film. In this study, we use the image analysis software ImageJ to process the SEM images and extract the peeling area for quantitative analysis. ImageJ is a public image processing software based on JAVA. The ImageJ software image-recognition process of the peeling area of the asphalt film is shown in Figure 9, and the peeling area after the ImageJ image processing is shown in Figure 10 and Table 1.

The percentage of the peeling area of the asphalt film of the samples with different porosities increases with the number of freeze-thaw cycles. The peeling area of the asphalt film on the mixture with a porosity of 24% has the largest increment, and the peeling speed of the asphalt film is also the fastest. As can be seen in Figures 6–8, the SEM image analysis of the specimens from the time of nonfreezing and thawing revealed that the raised aggregate content on the asphalt interface is higher than that with porosities of 19% and 21%. The main reason is that the asphalt membrane with a porosity of 24% peeled off a large area around a large number of raised aggregates, and the peeling area is greater than that with porosities of 19% and 21%. Thereafter, with an increase in the number of freeze-thaw cycles, the asphalt membrane and the peeling of the asphalt film intensified. After 20 freeze-thaw cycles, the peeling area of the asphalt film with a porosity of 24% reaches a maximum of 92.06%. The percentages of the peeling area of the asphalt film with

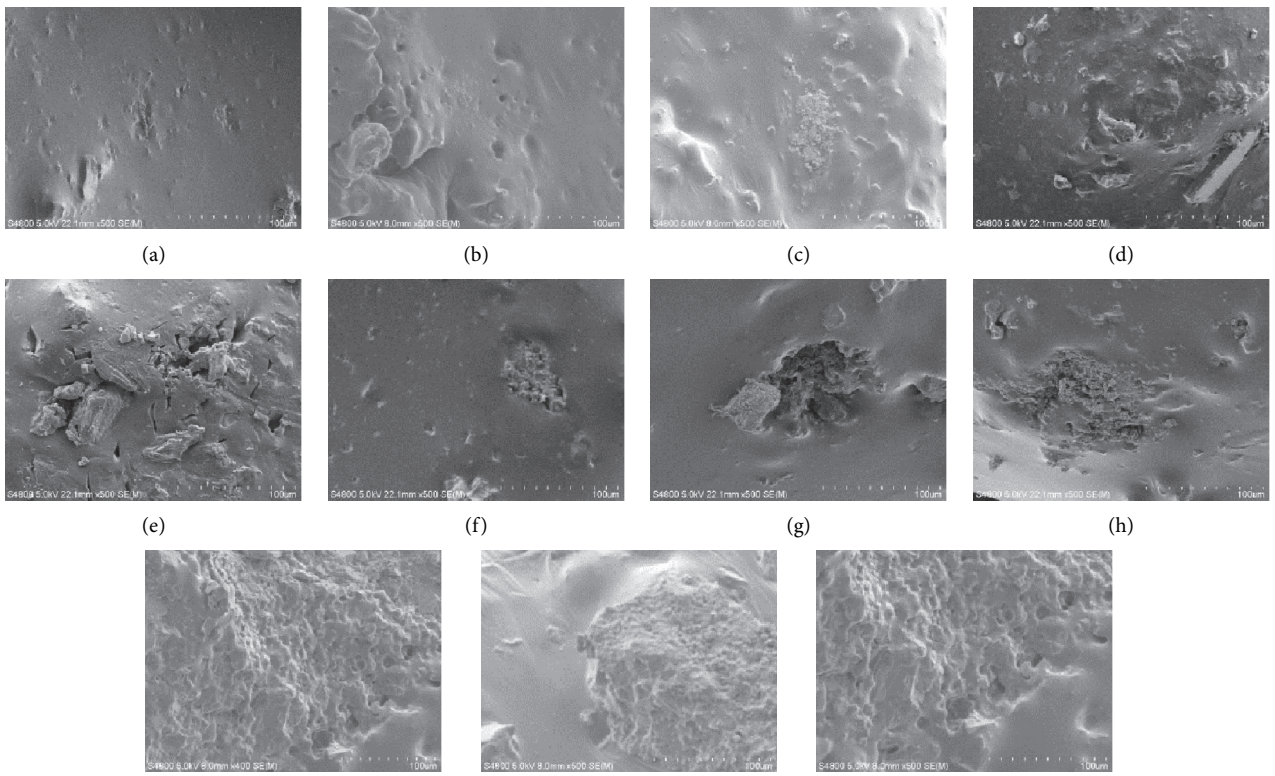

(a) (b) (c) (d)

(e) (f) (g) (h)

(i) (j) (k)

Figure 6: SEM images of PAC with a porosity of 19% after multiple freeze-thaw cycles. (a) No freezing-thawing. (b) 2 cycles. (c) 4 cycles. (d) 6 cycles. (e) 8 cycles. (f) 10 cycles. (g) 12 cycles. (h) 14 cycles. (i) 16 cycles. (j) 18 cycles. (k) 20 cycles.

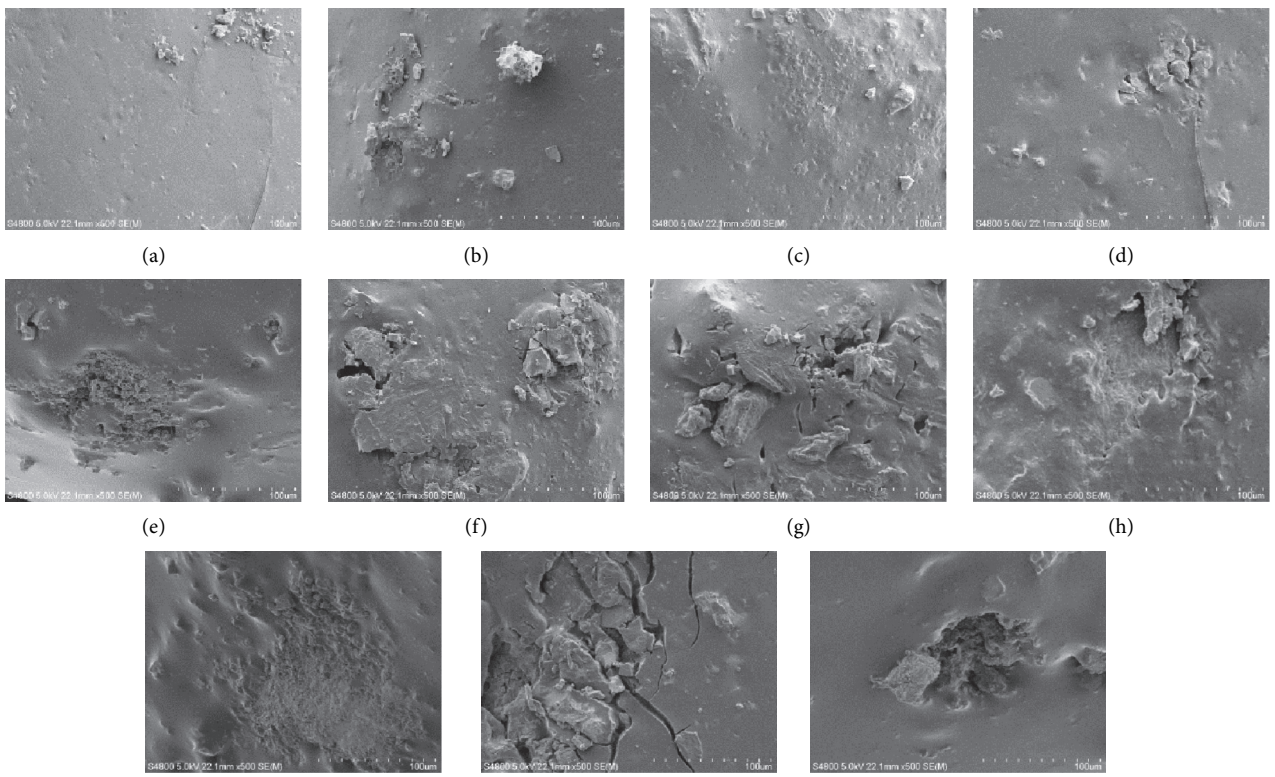

(a) (b) (c) (d)

(e) (f) (g) (h)

(i) (j) (k)

Figure 7: SEM images of PAC with a porosity of 21% after multiple freeze-thaw cycles. (a) No freezing-thawing. (b) 2 cycles. (c) 4 cycles. (d) 6 cycles. (e) 8 cycles. (f) 10 cycles. (g) 12 cycles. (h) 14 cycles. (i) 16 cycles. (j) 18 cycles. (k) 20 cycles.

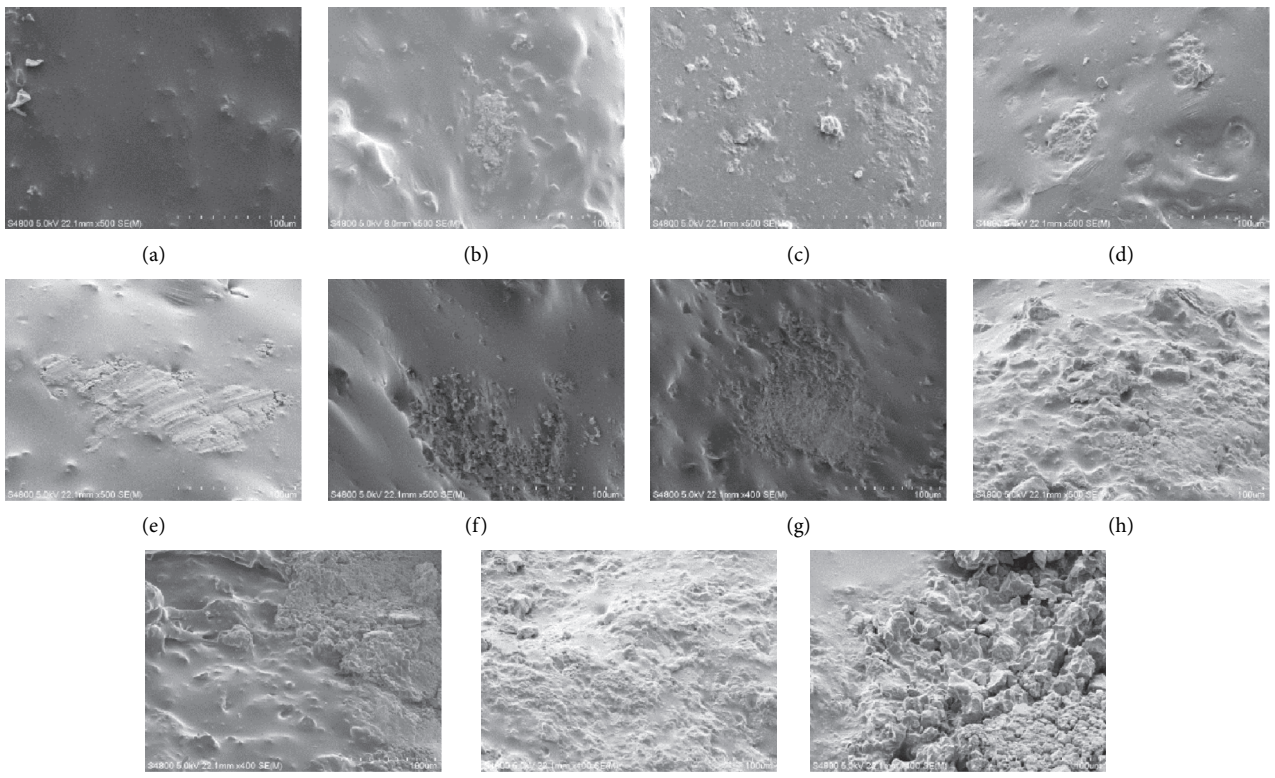

Figure 8: SEM images of PAC with a porosity of 24% after multiple freeze-thaw cycles. (a) No freezing-thawing. (b) 2 cycles. (c) 4 cycles. (d) 6 cycles. (e) 8 cycles. (f) 10 cycles. (g) 12 cycles. (h) 14 cycles. (i) 16 cycles. (j) 18 cycles. (k) 20 cycles.

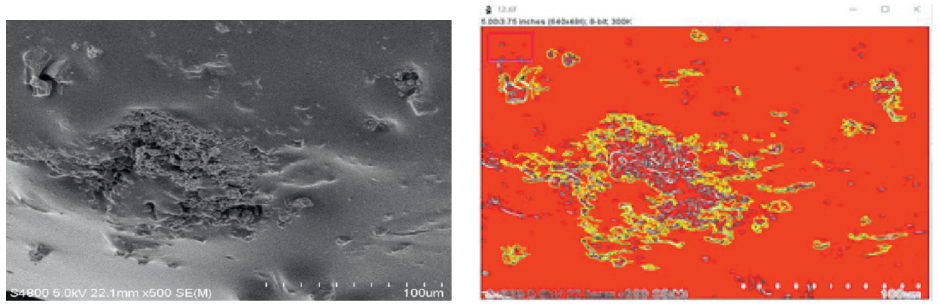

Figure 9: ImageJ software image-recognition process of the asphalt film peeling area. (a) Original SEM image. (b) Peeling surface recognition after ImageJ image processing.

porosities of 19% and 21% are roughly the same. Among them, the peeling area percentage of the asphalt film with a porosity of 21% is slightly better than that with a porosity of 19%, confirming that the mixture with a porosity ranging from 19% to 21% has the best freeze-thaw resistance.

The SEM experiment shows that as the number of freeze-thaw cycles and porosity increase, the freeze-thaw effect becomes increasingly significant, the asphalt becomes hard and brittle, and the temperature stress between asphalt and aggregate increases. Simultaneously, under the frost-heaving force of ice, it is easier to peel off with aggregate and crack.

4. Gray-Markov Prediction

4.1. Prediction of the PAC Water Stability Using the Gray-Markov Model. According to the characteristics of PAC in the seasonally frozen area, the balance of the road performance was considered, PAC with a porosity of 21% was selected, and the gray prediction of its water stability performance was performed. Based on the TSR of different freeze-thaw cycles, the GM (1, 1) model was established. The PAC water stability was predicted by the model after multiple freeze-thaw cycles. The specific calculation steps are as follows:

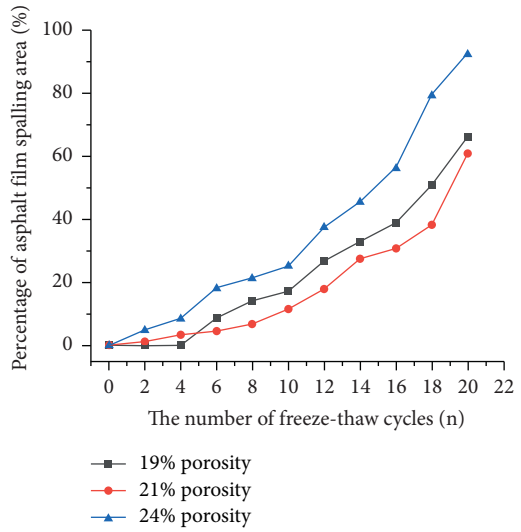

Figure 10: Peeling area changes of the asphalt film with the number of freeze-thaw cycles.

Table 1: Percentage of the asphalt film spalling area of the samples with different porosities under multiple freeze-thaw cycles.

Number of freeze-thaw cycles	Porosity rate		
	19%	21%	24%
0	0	0	0
2	0	1.17	4.78
4	0	3.39	8.38
6	8.65	4.50	18.08
8	14.13	6.83	21.22
10	17.25	11.48	25.09
12	26.71	17.72	37.37
14	32.78	27.38	45.36
16	38.84	30.71	56.05
18	50.77	38.15	79.11
20	66.07	60.79	92.07

(1) Constructing the original data series:

$$X_{(i)} = (100, 78.45, 73.47, 68.94, 65.31, 62.08, 59.18, 57.76, 53.13). \tag{15}$$

(2) Accumulating the processed data sequence:

$$Y_{(k)} = (100, 178.45, 251.92, 320.86, 386.17, 448.25, 507.43, 565.19, 618.32). \tag{16}$$

(3) Constructing the data vector Y and data matrix B:

$$Y_N = (78.45, 73.47, 68.94, 65.31, 62.08, 59.18, 57.76, 53.13)^{\mathrm{T}},$$
$$B^{\mathrm{T}} = \begin{bmatrix} -139.225 & -215.185 & -286.39 & -353.515 & -417.21 & -477.84 & -536.31 & -591.755 \\ 1 & 1 & 1 & 1 & 1 & 1 & 1 & 1 \end{bmatrix}. \tag{17}$$

(4) Using MATLAB to determine the parameters:

$$a = 0.0534, b = 84.9462. \tag{18}$$

The gray prediction equation of the TSR is as follows:

$$Y_{(k+1)} = \left(100 - \frac{84.9462}{0.0534}\right) e^{-0.0534k} + \frac{84.9462}{0.0534}. \tag{19}$$

(5) According to the predicted value $\hat{X}_{(k)}$ obtained by the GM(1, 1) model, the corresponding residual and its relative value were obtained. The residual relative value was used to divide it into the three states, $E_1 = (-1.83\%, -1\%]$, $E_2 = (-1\%, 1\%)$, and $E_3 = [1\%, 2.59\%)$. Among them, the left interval point of the E_1 state and the right interval point of the E_3 state were the minimum and maximum values of the residual relative values, respectively. Table 2 shows the state of the sequence of the residual relative values.

(6) Calculating the one-step transition probability matrix according to the state of the residual relative value sequence:

$$P = \left(P_{ij}\right)_{3\times 3} = \begin{pmatrix} \frac{2}{3} & \frac{1}{3} & 0 \\ \frac{1}{3} & 0 & \frac{2}{3} \\ \frac{1}{2} & \frac{1}{2} & 0 \end{pmatrix}. \tag{20}$$

The Markov test on the sequence was performed, and the marginal probability value $P_{\cdot j}$ was calculated, as shown in Table 3. The chi-square value was used to test the correlation of the test data, and the Markov model was based on the state transition matrix. The prediction result was only related to the immediately preceding state. The accuracy of the data prediction was crucial for the data correlation. Among them, the significance level α was 0.1, which implies that the sample probability replacing the overall sample is 90%. For this reason, the correlation coefficient significance level α was 0.1, according to the chi-square test threshold table $\chi^2_{0.1}(4) = 7.7794$. The statistics $\chi^2 = 7.8466$ and $\chi^2 > \chi^2_{0.1}(4)$ were calculated satisfying the Markov model, as shown in Table 4.

4.2. Model Accuracy Analysis. The specific steps for calculating the TSRs for 18 and 20 freeze-thaw cycles of PAC were as follows:

(1) After the transfer matrix was determined, the state of the next freeze-thaw cycle could be predicted based on the state of a certain number of freeze-thaw cycles. The relative value of the residuals with 16 freeze-thaw cycles was in the state of 1; thus, the initial vector of the relative value was $v_0 = (1, 0, 0)$. The state distribution after 18 freeze-thaw cycles from the one-step transition probability was

$$I^{(18)} = v_0 P = (1, 0, 0) \begin{pmatrix} \frac{2}{3} & \frac{1}{3} & 0 \\ \frac{1}{3} & 0 & \frac{2}{3} \\ \frac{1}{2} & \frac{1}{2} & 0 \end{pmatrix} = \left(\frac{2}{3}, \frac{1}{3}, 0\right). \tag{21}$$

Therefore, when the freeze-thaw cycle number was 18, the residual state of the TSR was max, = (2/3, 1/3, 0), and the state was E_1: $(-1.83\%, -1\%]$. The measured TSR for 18 freeze-thaw cycles was 49.43%. The predicted value from the GM(1, 1) model was 50.56%. The predicted value was corrected using equation (18); the corrected value was 49.85%.

The relative error was 2.29% when the gray model GM(1, 1) was used to calculate the TSR for 18 freeze-thaw cycles. The Markov model was used to correct it. By calculating and fitting, the average relative error was 0.85%. Compared with the error obtained with the GM(1, 1) model, the accuracy of the Gray-Markov model improved to 62.88%.

(2) Calculate the two-step transition probability matrix as

$$I^{(20)} = v_0 P^2 = (1, 0, 0) \begin{pmatrix} \frac{5}{9} & \frac{2}{9} & \frac{2}{9} \\ \frac{5}{9} & \frac{4}{9} & 0 \\ \frac{1}{2} & \frac{1}{6} & \frac{1}{3} \end{pmatrix} = \left(\frac{5}{9}, \frac{2}{9}, \frac{2}{9}\right). \tag{22}$$

Therefore, when the number of freeze-thaw cycles was 20, the residual state of the TSR was max, = (5/9, 2/9, 2/9), and the state was E_1: $(-1.83\%, -1\%]$. The measured TSR for 20 freeze-thaw cycles was 46.83%. The predicted value from the GM(1, 1) model using equation (20) was 47.94%. The predicted value was corrected using equation (18); the corrected value was 47.27%.

When the GM(1, 1) model was used to calculate the TSR for 20 freeze-thaw cycles, the relative error was 2.37%. The Markov model was used to correct it. By calculating and fitting, the average relative error was 0.93%. Compared with the error obtained with the GM(1, 1) model, the accuracy of the Gray-Markov model was improved to 60.76%.

Table 2: Status of the residual relative value sequence.

Number of freeze-thaw cycles	Measured value (%)	GM(1, 1) predictive value (%)	Residual $q(k)$ (%)	Residual relative value $\varepsilon(k)$ (%)	Status
0	100	100	0	0	2
2	78.45	77.52	0.93	1.19	3
4	73.47	73.49	−0.02	−0.03	2
6	68.94	69.66	−0.72	−1.04	1
8	65.31	66.04	−0.73	−1.12	1
10	62.08	62.71	−0.63	−1.01	1
12	59.18	59.35	−0.17	−0.29	2
14	57.76	56.26	1.50	2.59	3
16	53.13	53.67	−0.54	−1.02	1

Table 3: Marginal probability values.

Status	1	2	3
Marginal probability value $p_{\cdot j}$	1/2	1/4	1/4

Table 4: Statistical calculation table.

Status	$f_{i1}\lvert\ln p_{i1}/p_{\cdot 1}\rvert$	$f_{i2}\lvert\ln p_{i2}/p_{\cdot 2}\rvert$	$f_{i3}\lvert\ln p_{i3}/p_{\cdot 3}\rvert$	Total
1	0.5754	0.2877	0	0.8631
2	0.4055	0	1.9616	2.3671
3	0	0.6931	0	0.6931
Total	0.9809	0.9808	1.9616	7.8466

Table 5: Classification of the PAC water stability grade.

TSR (%)	>85	70~85	70~60	60~50	<50
Rating	Excellent	Good	Medium	Worse	Worst
Repair type	—	—	Minor repair	Intermediate repair	Overhaul
Useful life	0–1	1–4	4–5	5–7	>7

The above analysis shows that the TSR value of PAC can be predicted accurately by dividing the road performance of asphalt mixture using the Gray-Markov state transfer matrix established with the relative residual value.

4.3. Model Application. The investigation of the water damage on permeable asphalt pavement revealed that although the water stability of the mixture satisfied the requirements of construction codes, water damage was inevitable. To this end, this paper refers to the water stability evaluation standard [26] for PAC. The Lottman test used TSR = 0.7 as the limit. If the value was greater than 0.7, the mixture was considered to have better resistance to water damage; otherwise, it was more prone to water damage. The specific evaluation criteria are listed in Table 5.

A suitable correspondence between the water damage due to the freeze-thaw process and the type of maintenance by the evaluation standard can be established for PAC. In the test process, the TSR of the test specimen with a porosity of 24% after 20 freeze-thaw cycles was lower than 50%, and the loose phenomenon also occurred. This showed that the internal ice expansion force of the test specimen reached the failure threshold of the asphalt-aggregate adhesion force, which needed to be overhauled.

5. Conclusion

In this research, freeze-thaw cycles and SEM images of PAC were studied. Based on these results, the Gray-Markov model was used to evaluate the PAC water stability. The main findings of this study can be summarized as follows:

(1) The TSR of the PAC had a preferable correlation with the number of freeze-thaw cycles. The TSR decreases significantly with an increase in the number of freeze-thaw cycles. A comparative analysis of the decline in the water damage resistance of PAC under different porosities indicated that the porosity of the mixture with excellent water stability was 19–21%.

(2) The SEM experiment explained the water damage resistance of PAC under different porosities from a microstructural perspective. The experiment showed that when the porosity is 24%, the peeling area of the asphalt film increases significantly compared with that when the porosity is 19% and 21%, resulting in a significant TSR decrease.

(3) Typically, the Gray-Markov model is used to predict the performance of asphalt pavements. This paper proposed its application for PAC performance prediction. The state was divided by the relative value

of the residual, and a method for determining the state of the transition matrix was developed.

(4) By associating the TSR of PAC with the prediction model, the future development of the system can be inferred in time based on state transitions. According to the predicted TSR value of PAC combined with the evaluation standard, the corresponding relationship between the freeze-thaw cycle water damage and the maintenance type can be established.

Data Availability

All data, models, and codes included in this study are available upon reasonable request to the corresponding author.

Conflicts of Interest

The authors declare that there are no conflicts of interest regarding the publication of this paper.

Acknowledgments

This research was supported by the General Project of Liaoning Provincial Department of Education (no. lnjc202014).

References

[1] M. Zhang, C. Guo, B. Yu, Y. Yang, and Z. Lu, "CTCP temperature fields and stresses," *International Journal of Pavement Research and Technology*, vol. 10, no. 6, pp. 553–562, 2017.

[2] Y. Dong, Y. Tan, H. Liu, and L. Yang, "Noise performance of drainage asphalt pavement," *International Journal Pavement Research Technology*, vol. 2, no. 6, pp. 280–283, 2009.

[3] J. Shao, P. J. Lister, and A. McDonald, "A surface-temperature prediction model for porous asphalt pavement and its validation," *Meteorological Applications*, vol. 1, no. 2, pp. 129–134, 1994.

[4] W. S. Wang, Y. C. Cheng, G. R. Ma, G. J. Tan, X. Sun, and S. T. Yang, "Further investigation on damage model of eco-friendly basalt fiber modified asphalt mixture under freeze-thaw cycles," *Applied Sciences*, vol. 9, no. 1, 60 pages, 2019.

[5] L. Lisa, B. Romain, and K. Niki, "A thermodynamics-based model for freeze-thaw damage in asphalt mixtures," *International Journal of Solids and Structures*, vol. 203, pp. 264–275, 2020.

[6] Q. Guo, G. Li, Y. Gao et al., "Experimental investigation on bonding property of asphalt-aggregate interface under the actions of salt immersion and freeze-thaw cycles," *Construction and Building Materials*, vol. 206, pp. 590–599, 2019.

[7] H. Cai, "Discussion on the design method of modified pac-asphalt mixture mix," *International Journal of Civil Engineering and Machinery Manufacture*, vol. 5, no. 1, pp. 42–46, 2020.

[8] W. S. Wang, G. J. Tan, C. Y. Liang, Y. Wang, and Y. C. Cheng, "Study on viscoelastic properties of asphalt mixtures incorporating SBS polymer and basalt fiber under freeze-thaw cycles," *Polymers*, vol. 12, no. 8, 1804 pages, 2020.

[9] M. A. Vargas, L. Moreno, R. Montiel et al., "Effects of montmorillonite (Mt) and two different organo-Mt additives on the performance of asphalt," *Applied Clay Science*, vol. 139, pp. 20–27, 2017.

[10] F. Zhang and C. Hu, "Preparation and properties of high viscosity modified asphalt," *Polymer Composites*, vol. 38, no. 5, pp. 936–946, 2017.

[11] S. Wang, K. Aihong, X. Peng, L. Bo, W. Fu, and N. Jose, "Investigating the effects of chopped basalt fiber on the performance of porous asphalt mixture," *Advances in Materials Science and Engineering*, vol. 201912 pages, 2019.

[12] B. Xu, H. C. Dan, and L. Li, "Temperature prediction model of asphalt pavement in cold regions based on an improved BP neural network," *Applied Thermal Engineering*, vol. 120, pp. 568–580, 2017.

[13] B. Saghafi, A. Hassani, R. Noori, and M. G. Bustos, "Artificial neural networks and regression analysis for predicting faulting in jointed concrete pavements considering base condition," *International Journal of Pavement Research and Technology*, vol. 2, no. 1, pp. 20–25, 2009.

[14] E. S. Park, R. E. Smith, T. J. Freeman, and C. H. Spiegelman, "A Bayesian approach for improved pavement performance prediction," *Journal of Applied Statistics*, vol. 35, no. 11, pp. 1219–1238, 2008.

[15] J. C. Du and S. A. Cross, "Cold in-place recycling pavement rutting prediction model using grey modeling method," *Construction and Building Materials*, vol. 21, no. 5, pp. 921–927, 2006.

[16] K. A. Abaza, "Back-calculation of transition probabilities for Markovian-based pavement performance prediction models," *International Journal of Pavement Engineering*, vol. 17, no. 3, pp. 253–264, 2016.

[17] H. Baik, H. Jeong, and D. Abraham, "Estimating transition probabilities in Markov chain-based deterioration models for management of wastewater systems," *Journal of Water Resources Planning and Management*, vol. 132, no. 1, pp. 15–24, 2006.

[18] G. Morcous, "Performance prediction of bridge deck systems using Markov chains," *Journal of Performance of Constructed Facilities*, vol. 20, no. 2, pp. 146–155, 2006.

[19] K. Kobayashi, M. Do, and D. Han, "Estimation of Markovian transition probabilities for pavement deterioration forecasting," *KSCE Journal of Civil Engineering*, vol. 14, no. 3, pp. 343–351, 2010.

[20] S. G. Coles, J. A. Tawn, and R. L. Smith, "A seasonal Markov model for extremely low temperatures," *Environmetrics*, vol. 5, no. 3, pp. 221–239, 1994.

[21] C. Y. Sung and Y. I. Kim, "Void ratio and durability properties of porous polymer concrete using recycled aggregate with binder contents for permeability pavement," *Journal of Applied Polymer Science*, vol. 126, no. S2, pp. E338–E348, 2012.

[22] Y. Xue, S. Wu, H. Hou, and J. Zha, "Experimental investigation of basic oxygen furnace slag used as aggregate in asphalt mixture," *Journal of Hazardous Materials*, vol. 138, no. 2, pp. 261–268, 2006.

[23] P. Buddhavarapu, A. F. Smit, and J. A. Prozzi, "A fully Bayesian before–after analysis of permeable friction course (PFC) pavement wet weather safety," *Accident Analysis & Prevention*, vol. 80, pp. 89–96, 2015.

[24] Y. Cheng, C. Chai, C. Liang, and Y. Chen, "Mechanical performance of warm-mixed porous asphalt mixture with steel slag and crumb-rubber–SBS modified bitumen for seasonal frozen regions," *Materials*, vol. 12, no. 6, 857 pages, 2019.

[25] Y. Cheng, D. Yu, G. Tan, and C. Zhu, "Low-temperature performance and damage constitutive model of eco-friendly

basalt fiber–diatomite-modified asphalt mixture under freeze–thaw cycles," *Materials*, vol. 11, no. 11, 2148 pages, 2018.

[26] N. Xie, M. Akin, and X. Shi, "Permeable concrete pavements: a review of environmental benefits and durability," *Journal of Cleaner Production*, vol. 210, pp. 1605–1621, 2019.